



# Brain morphological and functional features in cognitive subgroups of schizophrenia

Yuka Yasuda, MD, PhD <sup>1,2,3</sup> Naohiro Okada, MD, PhD <sup>4,5</sup> Kiyotaka Nemoto, MD, PhD <sup>6</sup> Masaki Fukunaga, PhD,<sup>7</sup> Hidenaga Yamamori, MD, PhD,<sup>2,8,9</sup> Kazutaka Ohi, MD, PhD,<sup>10,11</sup> Daisuke Koshiyama, MD, PhD,<sup>4</sup> Noriko Kudo, PhD,<sup>2</sup> Tomoko Shiino, PhD,<sup>2</sup> Susumu Morita, MD,<sup>4,5</sup> Kentaro Morita, MD, PhD,<sup>4</sup> Hirotsugu Azechi, PhD,<sup>2</sup> Michiko Fujimoto, MD, PhD,<sup>2,9</sup> Kenichiro Miura, PhD,<sup>2</sup> Yoshiyuki Watanabe, MD, PhD,<sup>12</sup> Kiyoto Kasai, MD, PhD<sup>4,5</sup> and Ryota Hashimoto, MD, PhD <sup>2,3,9\*</sup>

**Aim:** Previous studies have reported different brain morphologies in different cognitive subgroups of patients with schizophrenia. We aimed to examine the brain structures and functional connectivity in these cognitive subgroups of schizophrenia.

**Methods:** We compared brain structures among healthy controls and cognitively deteriorated and preserved subgroups of patients with schizophrenia according to the decline in IQ. Connectivity analyses between subcortical regions and other brain areas were performed using resting-state functional magnetic resonance imaging among the groups.

**Results:** Whole brain and total cortical gray matter, right fusiform gyrus, left pars orbitalis gyrus, right pars triangularis, left superior temporal gyrus and left insula volumes, and bilateral cortical thickness were decreased in the deteriorated group compared to the control and preserved groups. Both schizophrenia subgroups had increased left lateral ventricle, right putamen and left pallidum, and decreased bilateral hippocampus, left precentral gyrus, right

rostral middle frontal gyrus, and bilateral superior frontal gyrus volumes compared with controls. Hyperconnectivity between the thalamus and a broad range of brain regions was observed in the deteriorated group compared to connectivity in the control group, and this hyperconnectivity was less evident in the preserved group. We also found hyperconnectivity between the accumbens and the superior and middle frontal gyri in the preserved group compared with connectivity in the deteriorated group.

**Conclusion:** These findings provide evidence of prominent structural and functional brain abnormalities in deteriorated patients with schizophrenia, suggesting that cognitive subgroups in schizophrenia might be useful biotypes to elucidate brain pathophysiology for new diagnostic and treatment strategies.

**Keywords:** brain functional connectivity, brain morphology, cognitive decline, cognitive subgroup, schizophrenia.

<http://onlinelibrary.wiley.com/doi/10.1111/pcn.12963/full>

Patients with schizophrenia display cognitive deficits in various kinds of neuropsychological tasks. It has been reconceptualized that cognitive impairments across domains that share a common neurobiological source may lead to ‘generalized’ or ‘global’ cognitive impairments, not specific impairments, in schizophrenia.<sup>1,2</sup> Decades of research have revealed that cognitive impairment is a prominent aspect of the psychopathology of schizophrenia.<sup>3</sup> Cognitive impairment is a critical determinant of quality of life and social function in people with this disorder, possibly playing a more substantial role than the severity of symptoms such as hallucinations and delusions.<sup>4–8</sup> Moreover, studies have suggested that cognitive impairment can also be a marker of outcome prediction for the prodromal

or initial stages of the illness. However, it is difficult to elucidate the pathology of cognitive impairment because of the heterogeneity of schizophrenia.<sup>7,9</sup> As understanding the mechanisms of cognitive impairments in schizophrenia is expected to contribute to treatment,<sup>10</sup> cognitive function is included as a dimensional assessment in the diagnostic criteria (DSM-5) to highlight the potential need for treatment and to specifically target cognitive remediation.<sup>1</sup>

Cognitive impairments in psychotic disorders have been reported to be related to brain structures, such as prefrontal and temporolimbic regions.<sup>11–14</sup> Brain volume alterations, such as larger ventricles, decreased gray matter and white matter volume, and alterations in insula, thalamus, and anterior cingulate cortex volume, have been

<sup>1</sup> Life Grow Brilliant Mental Clinic, Medical Corporation Foster, Osaka, Japan

<sup>2</sup> Department of Pathology of Mental Diseases, National Institute of Mental Health, National Center of Neurology and Psychiatry, Tokyo, Japan

<sup>3</sup> Molecular Research Center for Children’s Mental Development, United Graduate School of Child Development, Osaka University, Osaka, Japan

<sup>4</sup> Department of Neuropsychiatry, Graduate School of Medicine, The University of Tokyo, Tokyo, Japan

<sup>5</sup> World Premier International-International Research Center for Neurointelligence (WPI-IRCN), The University of Tokyo Institutes for Advanced Study (UTIAS), The University of Tokyo, Tokyo, Japan

<sup>6</sup> Department of Psychiatry, Faculty of Medicine, University of Tsukuba, Ibaraki, Japan

<sup>7</sup> Division of Cerebral Integration, National Institute for Physiological Sciences, Okazaki, Japan

<sup>8</sup> Japan Community Health Care Organization (JCHO), Osaka, Japan

<sup>9</sup> Department of Psychiatry, Osaka University Graduate School of Medicine, Osaka, Japan

<sup>10</sup> Department of Neuropsychiatry, Kanazawa Medical University, Ishikawa, Japan

<sup>11</sup> Medical Research Institute, Kanazawa Medical University, Ishikawa, Japan

<sup>12</sup> Department of Future Diagnostic Radiology, Osaka University Graduate School of Medicine, Osaka, Japan

\* Correspondence: Email: ryotahashimoto55@ncnp.go.jp

commonly identified in schizophrenia.<sup>15</sup> The Enhancing Neuro Imaging Genetics through Meta-Analysis (ENIGMA) Consortium<sup>16</sup> and a Japanese consortium, the Cognitive Genetics Collaborative Research Organization (COCORO),<sup>17</sup> independently revealed smaller-than-normal hippocampal, amygdalar, thalamic, and accumbal volumes, as well as a smaller-than-normal intracranial volume in schizophrenia. The possible clinical significance of these structural abnormalities in subcortical regions in schizophrenia has recently been reported as an association between hippocampal and accumbal volumes and memory function<sup>18</sup> and the relationship between the right thalamic volume and cognitive deficits and social function.<sup>19</sup> In a diffusion tensor imaging study, structural connectivity in right frontal white matter and the corpus callosum was revealed to be related to social function in schizophrenia.<sup>20</sup> These findings suggest that cognitive impairments are related to alterations in brain structures in patients with schizophrenia.

As schizophrenia is a heterogeneous mental disorder, it is desirable to perform subgroup classification to elucidate the pathophysiology and development of new diagnostic and treatment methods. Cognitive impairment, one of the core features of schizophrenia, has been suggested to be useful for classifying subgroups.<sup>1,3,21</sup> Weickert *et al.*<sup>22</sup> reported a variety of intellectual impairment patterns in patients with schizophrenia, including intellectual decline (deteriorated), preserved abilities (preserved), and premorbid deficits (compromised). This variability seems to suggest potential heterogeneity in the neuropathology of schizophrenia based on cognitive status. Furthermore, the following two studies reported that there were different alterations in brain structures in patients with schizophrenia classified according to these cognitive subgroups.<sup>23,24</sup> Czepielewski *et al.*<sup>23</sup> showed that patients with schizophrenia with a compromised IQ had smaller-than-normal total brain volume, intracranial volume, total brain volume corrected for intracranial volume, cortical gray matter volume, cortical thickness, and insula volume. They also reported that patients with schizophrenia with a preserved IQ showed reduced cortical gray matter volume and cortical thickness.<sup>23</sup> Weinberg *et al.*<sup>24</sup> reported that patients with schizophrenia had significantly reduced inferior parietal volume compared to that of healthy controls (HC). The severely deteriorated schizophrenia group showed significantly reduced total hippocampus, precuneus, lingual gyrus, and superior temporal gray matter volumes relative to those of the preserved group.<sup>24</sup> In this way, the cognitive subgroups of people with schizophrenia according to a decline in IQ could be underpinned by different brain morphologies.<sup>22</sup> However, the relationship between brain physiology and subgroups of patients with schizophrenia based on IQ decline has not yet been elucidated. In this study, we aimed to comprehensively replicate differential structural alterations based on the IQ decline in subgroups of patients with schizophrenia in a larger population and to examine whether the differential alterations in brain structures influence the functional brain connectivity across these subgroups of schizophrenia based on IQ decline.

## Methods

### Participants

The subjects consisted of 171 patients with schizophrenia (60 for brain connectivity analysis) and 633 HC (234 for brain connectivity analysis). Diagnostic and exclusion criteria have been described previously.<sup>19,25</sup> Written informed consent was obtained from all subjects after the procedures had been fully explained.

The study was performed in accordance with the World Medical Association's Declaration of Helsinki and was approved by the Research Ethical Committee of Osaka University. All participants provided written consent to the study after full explanation of the study procedures. Anonymity was preserved for all participants.

### Cognitive measures and other measures

All participants were administered the full-scale Wechsler Adult Intelligence Scale –III (WAIS-III)<sup>26</sup> to obtain their current IQ and the Japanese version of the National Adult Reading Test 50 (JART)<sup>27</sup> to obtain an estimated premorbid IQ score. The Wechsler Memory Scale – Revised<sup>28</sup> was administered to assess the memory functioning of the participants. Current symptoms of schizophrenia were evaluated using the Positive and Negative Syndrome Scale (PANSS).<sup>29</sup> Daily doses of antipsychotics, expressed as the chlorpromazine equivalent (CPZeq), in patients were calculated according to previous literature.<sup>30</sup>

### Classification of IQ decline subgroups

Based on previous findings,<sup>22</sup> we classified patients with schizophrenia into three groups: (i) deteriorated, those displaying a meaningful decline in IQ ( $\geq 10$  points) as evidenced by the difference between current IQ (based on the full-scale IQ score of the WAIS-III) and estimated premorbid IQ score (based on the JART score); (ii) preserved, those having an estimated premorbid IQ score above 90 and less than a 10-point difference between their estimated premorbid IQ and their current IQ; and (iii) compromised, those displaying an estimated premorbid IQ score below 90 and less than a 10-point difference between their estimated premorbid IQ and their current IQ. The existence of a 10-point IQ decline took precedence over either of the cutoff strategies described. The numbers in each group were as follows: deteriorated,  $n = 111$  (65%); preserved,  $n = 54$  (32%); and compromised,  $n = 6$  (4%) (Fig. S1). As the compromised group was too small ( $n = 6$ ), we excluded this group from the analysis.

### Statistical analysis for demographics and clinical characteristics

Statistical analyses were performed using SPSS for Windows Version 24 (SPSS Japan Inc., Tokyo, Japan). Group comparisons of sex were performed using the  $\chi^2$ -test. We performed *t*-tests to compare clinical characteristics between preserved and deteriorated groups, and analysis of variance (ANOVA) was employed for comparisons of continuous variables, as appropriate. For defining statistical significance, we set the type I error rate (*P*-value) at 0.05. Cohen's *d* effect sizes were calculated from the overall group contrast.

### Structural and functional imaging and volumetric and connectivity processing

We performed magnetic resonance imaging (MRI) and obtained T1-weighted images with two different scanners: Osaka A and Osaka B. We scanned 109 patients (deteriorated,  $n = 70$ ; preserved,  $n = 34$ ; and compromised,  $n = 5$ ) and 399 HC with Osaka A; and 62 patients (deteriorated,  $n = 41$ ; preserved,  $n = 20$ ; and compromised,  $n = 1$ ) and 234 HC with Osaka B. The scanner type for Osaka A was a GE 1.5 T, Signa EXCITE. T1-weighted images, using a fast-spoiled gradient echo (SPGR) and a head QD coil, were acquired with the following parameters: repetition time (TR) = 12.6 ms, echo time (TE) = 4.2 ms, inversion time (TI) = 400 ms, flip angle = 15 degrees, matrix =  $256 \times 256 \times 124$ , field of view (FOV) =  $240 \times 240 \times 172$  mm, voxel size =  $0.9375 \times 0.9375 \times 1.4$  mm, slice thickness = 1.4 mm, and number of slices = 124. The slice orientation was in the sagittal plane. The scanner type for Osaka B was a GE 3.0 T, Signa HDxt. T1-weighted images, using a fast SPGR and an 8HRBRAIN coil, were acquired with the following parameters: TR = 7.2 ms, TE = 2.9 ms, TI = 400 ms, flip angle = 11 degrees, matrix =  $256 \times 256 \times 172$ , FOV =  $240 \times 240 \times 172$  mm, voxel size =  $0.9375 \times 0.9375 \times 1$  mm, slice thickness = 1 mm, and number of slices = 172. The slice orientation was in the sagittal plane.

We performed structural image processing in the same way as that performed in our previous study.<sup>17–19</sup> We checked original T1-weighted images through visual inspection for quality control. We excluded images with a low signal-to-noise ratio or any artifacts, those with partial deficits, and those with any abnormal organic findings. Next, we processed T1-weighted imaging data that had passed the first quality-control step with FreeSurfer software version 5.3

(<http://surfer.nmr.mgh.harvard.edu>).<sup>30</sup> Through this procedure, we obtained images showing the subcortical segmentation and regional volumes (for the hippocampus, amygdala, thalamus, nucleus accumbens, caudate, putamen, globus pallidus in both hemispheres, and the intracranial volume [ICV]). After that, two independent researchers visually inspected each segmentation image to exclude images with poor segmentation. No subject was excluded due to the failure of FreeSurfer processing. After these two quality-control steps, we obtained the raw subcortical volume data. The analytical methods used in the study by van Erp *et al.*<sup>16</sup> from ENIGMA-SZ were followed in this analysis. We employed the normalized regional volume to remove the effects of the confounding factors considering linear and nonlinear age effects on subcortical regional volumes as described previously.<sup>17–19</sup> We also extracted cortical thickness measures from both scanners using FreeSurfer 5.3 (<http://surfer.nmr.mgh.harvard.edu>). Cortical parcellations were created based on the Desikan–Killiany atlas, with a total of 68 (34 left and 34 right) cortical gray matter regions. Hemispheric average cortical thicknesses were also calculated. Based on the standardized ENIGMA protocols (<http://enigma.ini.usc.edu/protocols/imaging-protocols>), the segmentations were visually inspected by three independent researchers and statistically evaluated for outliers.

MRI scanning for resting-state fMRI (rs-fMRI) was performed on Osaka B, a GE 3.0T Signa HDxt using an 8HRBRAIN head coil. RsfMRI was acquired using a T2\* echo-planar imaging (EPI) sequence with the following parameters: TR/TE, 2000 ms/30 ms; flip angle, 90°; acquisition matrix, 64 × 64; FOV, 220 mm × 220 mm; voxel size, 3.44 mm × 3.44 mm × 3.50 mm; slice thickness, 3.50 mm; and slice gap, none. Each brain volume consisted of 40 axial slices, and each functional run contained 150 image volumes preceded by four dummy volumes. Participants were asked to stay awake, not to focus their thoughts on anything in particular, and to keep their eyes closed during rsfMRI scanning.

RsfMRI data preprocessing was performed with Data Processing Assistant for Resting-State fMRI Advanced Edition (DPARSF-A) version 2.1 software,<sup>31,32</sup> which is a MATLAB (MathWorks, Natick,

MA, USA) toolbox. Imaging data were adjusted for a temporal shift in acquisition, spatially realigned to the middle slice, nonlinearly normalized to the EPI MNI template (resulting in an isotropic voxel size of 3 × 3 × 3 mm), smoothed using a full-width at half-maximum kernel of 4 mm, and bandpass filtered (0.01–0.1 Hz). Nuisance signals from the head-motion time series estimated by the Friston 24-parameter model,<sup>33</sup> as well as signals from white matter and cerebrospinal fluid signals, were regressed out of each voxel's time course. Moreover, the head motion scrubbing regression was modeled using the following parameters: framewise displacement threshold for 'bad' time-points, 0.5; scrubbing time-points before 'bad' time-points, 1; and scrubbing time-points after 'bad' time-points, 2.<sup>34</sup> Finally, the time course data were processed for each voxel, as well as for each of the brain regions defined by the Harvard–Oxford atlas distributed with FSL (<http://www.fmrib.ox.ac.uk/fsl/>), by averaging over voxels within each region. Intraregional correlation coefficients indicating the extent of synchronicity were calculated between every pair of a subcortical region and a voxel, and connectivity maps were created. Correlation coefficients representing functional connectivity (FC) were converted to z-scores using Fisher's transformation.

**Statistical analysis for imaging data**

Statistical analyses were performed using spss for Windows Version 24 (SPSS Japan Inc., Tokyo, Japan). For each segmented structure, except for the ICV, a total of 798 subjects (633 controls, 111 patients with deteriorated IQ, and 54 patients with preserved IQ) were compared using analysis of covariance (ANCOVA), including age, sex, type of MRI scanner, and ICV as covariates. The ICV was analyzed using ANCOVA, including age, sex, and type of MRI scanner as covariates. Because there were 94 brain regions, statistical significance was defined at  $P < 5.3 \times 10^{-4}$ . All reported P-values are based on two-tailed tests. Post-hoc comparisons were performed after ANCOVA using the Bonferroni correction when there was a significant difference among the groups. Statistical significance was defined for post-hoc comparisons at  $P < 0.05$ . Cohen's *d* effect sizes were calculated between the groups.

**Table 1.** Demographic and cognitive characteristics of the participants

| Variables                            | SZ                              |                                   |                                  | Statistics                |   |   |  |  |         | Effect size |           |
|--------------------------------------|---------------------------------|-----------------------------------|----------------------------------|---------------------------|---|---|--|--|---------|-------------|-----------|
|                                      | D-IQ                            | P-IQ                              | HC                               | D-IQ–P-IQ–HC <sup>†</sup> |   | D-IQ–HC <sup>‡</sup>                      | P-IQ–HC <sup>‡</sup>                     | D-IQ–P-IQ <sup>‡</sup>                   | D-IQ–HC | P-IQ–HC     | D-IQ–P-IQ |
|                                      |                                 |                                   |                                  | $\chi^2/F$ -value         | P-value                                   |   |  |  |         |             |           |
| No. (%) with data, (male/female)     | <i>n</i> = 111 (64.9%), (61/50) | <i>n</i> = 54 (31.6%), (33/21) HC | <i>n</i> = 633 (100%), (315/318) | 3.27                      | 0.19                                      | –   | –  | –  | –       | –           | –         |
| Age, years                           | 34.3 (10.3)                     | 36.1 (13.8)                       | 34.1 (12.9)                      | 0.65                      | 0.52                                      | 1.0                                       | 0.76                                     | 1.0                                      | 0.02    | 0.15        | –0.15     |
| Years of education                   | 13.7 (2.3)                      | 14.4 (2.9)                        | 15.0 (2.1)                       | 19.42                     | <b><math>5.8 \times 10^{-9}</math>*</b>   | <b><math>6.6 \times 10^{-9}</math>*</b>   | 0.10                                     | 0.16                                     | –0.62   | –0.26       | –0.27     |
| Estimated premorbid FIQ <sup>§</sup> | 101.2 (11.1)                    | 104.1 (7.0)                       | 108.5 (7.7)                      | 40.58                     | <b><math>1.7 \times 10^{-17}</math>*</b>  | <b><math>1.7 \times 10^{-16}</math>*</b>  | <b><math>6.5 \times 10^{-4}</math>*</b>  | 0.10                                     | –0.75   | –0.59       | –0.31     |
| WAIS FIQ                             | 78.8 (14.3)                     | 103.0 (11.6)                      | 111.9 (12.1)                     | 340.19                    | <b><math>1.8 \times 10^{-107}</math>*</b> | <b><math>8.8 \times 10^{-108}</math>*</b> | <b><math>1.6 \times 10^{-6}</math>*</b>  | <b><math>2.9 \times 10^{-29}</math>*</b> | –2.50   | –0.75       | –1.86     |
| WMS-R index                          |                                 |                                   |                                  |                           |   |   |  |  |         |             |           |
| No.                                  | <i>n</i> = 107                  | <i>n</i> = 53                     | <i>n</i> = 632                   |                           |   |   |  |  |         |             |           |
| Verbal memory                        | 76.6 (19.7)                     | 96.4 (17.6)                       | 112.2 (14.1)                     | 262.87                    | <b><math>3.3 \times 10^{-88}</math>*</b>  | <b><math>6.4 \times 10^{-86}</math>*</b>  | <b><math>3.2 \times 10^{-12}</math>*</b> | <b><math>7.0 \times 10^{-14}</math>*</b> | –2.08   | –0.99       | –1.06     |
| Visual memory                        | 79.0 (19.2)                     | 97.4 (13.0)                       | 105.2 (9.6)                      | 236.71                    | <b><math>3.0 \times 10^{-81}</math>*</b>  | <b><math>2.8 \times 10^{-81}</math>*</b>  | <b><math>7.8 \times 10^{-6}</math>*</b>  | <b><math>1.4 \times 10^{-19}</math>*</b> | –1.73   | –0.69       | –1.12     |
| General memory                       | 74.2 (19.2)                     | 96.3 (16.3)                       | 111.8 (13.3)                     | 321.92                    | <b><math>6.0 \times 10^{-103}</math>*</b> | <b><math>6.0 \times 10^{-101}</math>*</b> | <b><math>5.0 \times 10^{-13}</math>*</b> | <b><math>2.1 \times 10^{-18}</math>*</b> | –2.27   | –1.04       | –1.24     |
| Attention concentration              | 88.2 (14.4)                     | 100.8 (14.9)                      | 110.1 (12.8)                     | 131.64                    | <b><math>4.6 \times 10^{-50}</math>*</b>  | <b><math>4.6 \times 10^{-49}</math>*</b>  | <b><math>2.8 \times 10^{-6}</math>*</b>  | <b><math>5.7 \times 10^{-8}</math>*</b>  | –1.61   | –0.67       | –0.86     |
| Delayed recall                       | 71.9 (18.7)                     | 93.1 (16.9)                       | 109.5 (12.0)                     | 371.83                    | <b><math>1.7 \times 10^{-114}</math>*</b> | <b><math>9.6 \times 10^{-112}</math>*</b> | <b><math>3.4 \times 10^{-16}</math>*</b> | <b><math>2.0 \times 10^{-19}</math>*</b> | –2.39   | –1.11       | –1.19     |

The mean (SD) differences in values among individuals with SCZ who have deteriorated IQ, those who have preserved IQ, and HC.

<sup>†</sup>All values between the three groups, except for sex, were analyzed by ANOVA (Sex was analyzed by  $\chi^2$ -test).

<sup>‡</sup>Post-hoc comparisons were performed after ANOVA using a Bonferroni correction.

<sup>§</sup>FIQ measured by using Japanese Adult Reading Test.

\* $P < 0.05$  was considered significant. The Cohen's *d* effect sizes (*d*) are indicated. Significant differences are shown in bold.

FIQ, full-scale IQ; D-IQ, deteriorated IQ; HC, healthy controls; P-IQ, preserved IQ; SCZ, schizophrenia; WAIS-III, Wechsler Adult Intelligence Scale – III; WMS-R, Wechsler Memory Scale – Revised.

**Table 2.** Clinical characteristics of patients with SCZ

| Variables                                      | SCZ                           |                              | Statistics <sup>†</sup> |                               | Effect size<br><i>d</i> |
|--|-------------------------------|------------------------------|-------------------------|-------------------------------|-------------------------|
|  | D-IQ                          | P-IQ                         | <i>t</i> -value         | <i>P</i> -value               |                         |
| Age of onset, years, <i>n</i>                  | 23.0 (8.0), <i>n</i> = 111    | 24.7 (9.6), <i>n</i> = 54    | -1.21                   | 0.23                          | -0.195                  |
| Periods of illness, years, <i>n</i>            | 11.0 (8.2), <i>n</i> = 111    | 11.0 (9.6), <i>n</i> = 54    | -0.01                   | 0.99                          | -0.002                  |
| Global Assessment of Functioning, <i>n</i>     | 39.5 (12.8), <i>n</i> = 88    | 46.6 (17.3), <i>n</i> = 45   | -2.41                   | <b>1.9 × 10<sup>-2</sup>*</b> | -0.461                  |
| PANSS  |                               |                              |                         |                               |                         |
| PANSS Positive score, <i>n</i>                 | 19.6 (5.7), <i>n</i> = 110    | 18.1 (6.1), <i>n</i> = 53    | 1.60                    | 0.11                          | 0.265                   |
| PANSS Negative score, <i>n</i>                 | 21.4 (5.6), <i>n</i> = 110    | 17.4 (5.2), <i>n</i> = 53    | 4.44                    | <b>1.6 × 10<sup>-5</sup>*</b> | 0.753                   |
| PANSS General score, <i>n</i>                  | 45.1 (10.5), <i>n</i> = 110   | 39.6 (11.1), <i>n</i> = 53   | 3.09                    | <b>2.4 × 10<sup>-3</sup>*</b> | 0.511                   |
| PANSS total score, <i>n</i>                    | 86.2 (19.4), <i>n</i> = 110   | 75.1 (20.8), <i>n</i> = 53   | 3.34                    | <b>1.0 × 10<sup>-3</sup>*</b> | 0.553                   |
| Daily dose of CPZeq                            |                               |                              |                         |                               |                         |
| Total amount of CPZeq, <i>n</i>                | 725.7 (586.1), <i>n</i> = 111 | 471.9 (520.4), <i>n</i> = 54 | 2.71                    | <b>7.5 × 10<sup>-3</sup>*</b> | 0.458                   |
| CPZeq (typical antipsychotic drugs), <i>n</i>  | 101.9 (318.9), <i>n</i> = 111 | 11.0 (34.6), <i>n</i> = 54   | 2.97                    | <b>3.7 × 10<sup>-3</sup>*</b> | 0.401                   |
| CPZeq (atypical antipsychotic drugs), <i>n</i> | 623.9 (515.0), <i>n</i> = 111 | 460.9 (516.8), <i>n</i> = 54 | 1.91                    | <b>5.8 × 10<sup>-2</sup></b>  | 0.316                   |

The mean (SD) differences in the values among individuals with SCZ who have deteriorated IQ and those who have preserved IQ.

<sup>†</sup>*t*-test.

\**P* < 0.05 was considered significant. The Cohen's *d* effect sizes (*d*) are indicated. Significant differences are shown in bold.

CPZeq, chlorpromazine-equivalents; D-IQ, deteriorated IQ; PANSS, Positive and Negative Symptom Scale; P-IQ, preserved IQ; SCZ, schizophrenia.

**Table 3.** Whole brain structure comparisons among D-IQ and P-IQ patients with SCZ and HC

| Brain structures            | SCZ                 |                     |                     | Statistics                |                                |                                |                        |                               | Effect size     |                 |           |
|-----------------------------|---------------------|---------------------|---------------------|---------------------------|--------------------------------|--------------------------------|------------------------|-------------------------------|-----------------|-----------------|-----------|
|                             | D-IQ                | P-IQ                | HC                  | D-IQ–P-IQ–HC <sup>†</sup> |                                | D-IQ–HC <sup>‡</sup>           | P-IQ–HC <sup>‡</sup>   | D-IQ–P-IQ <sup>‡</sup>        | D-IQ–HC         | P-IQ–HC         | D-IQ–P-IQ |
|                             | <i>n</i> = 111      | <i>n</i> = 54       | <i>n</i> = 633      | <i>F</i> -value           | <i>P</i> -value                | <i>P</i> -value                | <i>P</i> -value        | <i>P</i> -value               | <i>P</i> -value | <i>P</i> -value | <i>d</i>  |
| ICV                         | 1470.52<br>(179.60) | 1489.62<br>(154.87) | 1478.26<br>(186.38) | 0.92                      | 0.40                           | 0.54                           | 1.0                    | 1.0                           | -0.04           | 0.07            | -0.11     |
| TBV                         | 1077.65<br>(113.00) | 1094.27<br>(115.11) | 1106.45<br>(123.06) | 13.78                     | <b>1.3 × 10<sup>-6</sup>*</b>  | <b>3.0 × 10<sup>-6</sup>*</b>  | 5.9 × 10 <sup>-2</sup> | 0.87                          | -0.24           | -0.10           | -0.15     |
| Whole brain gray matter     | 606.05<br>(67.29)   | 621.37<br>(65.82)   | 627.07<br>(76.15)   | 23.73                     | <b>9.8 × 10<sup>-11</sup>*</b> | <b>5.0 × 10<sup>-11</sup>*</b> | 0.30                   | <b>1.4 × 10<sup>-2</sup>*</b> | -0.29           | -0.08           | -0.23     |
| Total cortical gray matter  | 445.95<br>(51.71)   | 458.84<br>(50.47)   | 464.79<br>(59.89)   | 27.01                     | <b>4.5 × 10<sup>-12</sup>*</b> | <b>2.7 × 10<sup>-12</sup>*</b> | 0.17                   | <b>1.2 × 10<sup>-2</sup>*</b> | -0.34           | -0.11           | -0.25     |
| Subcortical gray matter     | 56.53<br>(5.85)     | 57.62<br>(5.43)     | 57.19<br>(5.98)     | 2.03                      | 0.13                           | 0.23                           | 1.0                    | 0.24                          | -0.11           | 0.08            | -0.19     |
| Total cortical white matter | 445.02<br>(51.73)   | 446.05<br>(57.34)   | 452.80<br>(54.14)   | 3.85                      | 2.2 × 10 <sup>-2</sup>         | 0.21                           | 6.7 × 10 <sup>-2</sup> | 1.0                           | -0.15           | -0.12           | -0.02     |
| Left cortical white matter  | 221.66<br>(25.70)   | 222.23<br>(28.52)   | 225.45<br>(26.76)   | 3.74                      | 2.4 × 10 <sup>-2</sup>         | 0.22                           | 7.3 × 10 <sup>-2</sup> | 1.0                           | -0.14           | -0.12           | -0.02     |
| Right cortical white matter | 223.36<br>(26.14)   | 223.82<br>(28.88)   | 227.35<br>(27.45)   | 3.90                      | 2.1 × 10 <sup>-2</sup>         | 0.20                           | 6.5 × 10 <sup>-2</sup> | 1.0                           | -0.15           | -0.13           | -0.02     |
| Left cortical thickness     | 2.41<br>(0.11)      | 2.44<br>(0.11)      | 2.46<br>(0.12)      | 21.13                     | <b>1.2 × 10<sup>-9</sup>*</b>  | <b>4.3 × 10<sup>-10</sup>*</b> | 1.0                    | <b>1.5 × 10<sup>-3</sup>*</b> | -0.45           | -0.14           | -0.32     |
| Right cortical thickness    | 2.40<br>(0.11)      | 2.44<br>(0.12)      | 2.46<br>(0.13)      | 21.39                     | <b>9.0 × 10<sup>-10</sup>*</b> | <b>3.4 × 10<sup>-10</sup>*</b> | 1.0                    | <b>3.6 × 10<sup>-3</sup>*</b> | -0.44           | -0.16           | -0.29     |

The mean (SD) differences in brain volume (cm<sup>3</sup>) or thickness (mm) among individuals with SCZ who have D-IQ or P-IQ and HC. All values, except for ICV, were analyzed with age, sex, ICV, and types of MRI machine as covariates (ICV was analyzed with age, sex and MRI machine as covariates).

<sup>†</sup>ANCOVA.

\**P* < 5.3 × 10<sup>-4</sup> was considered significant.

<sup>‡</sup>Post-hoc comparisons were performed after ANCOVA using a Bonferroni correction. When there were significant differences among the groups.

\**P* < 0.05 was considered significant. The Cohen's *d* effect sizes (*d*) are indicated. Significant differences are shown in bold.

D-IQ, deteriorated IQ; HC, healthy controls; ICV, intracranial volume; P-IQ, preserved IQ; SCZ, schizophrenia; TBV, total brain volume.

A total of 294 subjects (234 controls, 40 patients with deteriorated IQ, and 20 patients with preserved IQ) were analyzed for brain connectivity. The second-level analyses of seed-based FC maps were performed in *SPM12* (Wellcome Department of Cognitive Neurology, London, UK) running on *MATLAB R2014b*. We compared functional connectivity maps seeded in the bilateral thalamus, accumbens, amygdala, caudate nucleus, hippocampus, pallidum, and putamen between the deteriorated group and control group, the preserved group and control group, and the deteriorated group and preserved group controlling for age and sex. For the analysis of FC maps, the statistical threshold was set at an uncorrected  $P < 0.001$  at the voxel level and a family-wise-error-corrected  $P < 0.05$  at the cluster level.

**Results**

**Demographic, cognitive, and clinical characteristics**

There was no significant difference in sex and age among the three groups; however, ANOVA revealed significant differences in years of education, estimated premorbid FIQ (FIQ from the JART) and current FIQ (FIQ from the WAIS-III) among the three groups (Table 1). After post-hoc comparisons, the HC group had significantly more years of education than the deteriorated group, but there was no significant difference in years of education between the preserved group and either the control group or the deteriorated group (Table 1). Post-hoc comparison analyses also indicated that the HC group had higher estimated premorbid IQ scores than the preserved and deteriorated

**Table 4.** Subcortical brain volume comparisons among subgroups of subjects

| Regions                        | SCZ            |               |                | Statistics                |                                |                                |                               | Effect size                   |          |          |           |
|--------------------------------|----------------|---------------|----------------|---------------------------|--------------------------------|--------------------------------|-------------------------------|-------------------------------|----------|----------|-----------|
|                                | D-IQ           | P-IQ          | HC             | D-IQ–P-IQ–HC <sup>†</sup> |                                | D-IQ–HC <sup>‡</sup>           | P-IQ–HC <sup>‡</sup>          | D-IQ–P-IQ <sup>‡</sup>        | D-IQ–HC  | P-IQ–HC  | D-IQ–P-IQ |
|                                | <i>n</i> = 111 | <i>n</i> = 54 | <i>n</i> = 633 | <i>F</i> -value           | <i>P</i> -value                | <i>P</i> -value                | <i>P</i> -value               | <i>P</i> -value               | <i>d</i> | <i>d</i> | <i>d</i>  |
| Left lateral ventricle volume  | 10.04 (5.74)   | 9.48 (3.93)   | 7.75 (3.93)    | 22.01                     | <b>5.0 × 10<sup>-10*</sup></b> | <b>1.2 × 10<sup>-9*</sup></b>  | <b>2.3 × 10<sup>-2*</sup></b> | 0.30                          | 0.467    | 0.441    | 0.114     |
| Right lateral ventricle volume | 8.80 (5.12)    | 7.82 (3.40)   | 6.64 (3.26)    | 25.02                     | <b>2.9 × 10<sup>-11*</sup></b> | <b>2.0 × 10<sup>-11*</sup></b> | 0.14                          | <b>2.6 × 10<sup>-2*</sup></b> | 0.503    | 0.355    | 0.225     |
| Left thalamus volume           | 7.72 (1.09)    | 7.59 (1.12)   | 7.86 (1.21)    | 4.43                      | 1.2 × 10 <sup>-2</sup>         | 0.31                           | 2.4 × 10 <sup>-2</sup>        | 0.62                          | -0.121   | -0.233   | 0.119     |
| Right thalamus volume          | 6.88 (1.14)    | 6.99 (1.07)   | 7.07 (1.11)    | 4.68                      | 9.5 × 10 <sup>-3</sup>         | 8.9 × 10 <sup>-3</sup>         | 0.93                          | 0.98                          | -0.172   | -0.076   | -0.101    |
| Left caudate nucleus volume    | 3.67 (0.52)    | 3.85 (0.52)   | 3.69 (0.56)    | 4.24                      | 1.5 × 10 <sup>-2</sup>         | 1.0                            | 1.3 × 10 <sup>-2</sup>        | 2.8 × 10 <sup>-2</sup>        | -0.041   | 0.289    | -0.344    |
| Right caudate nucleus volume   | 3.55 (0.51)    | 3.71 (0.48)   | 3.52 (0.53)    | 5.11                      | 6.2 × 10 <sup>-3</sup>         | 1.0                            | 5.1 × 10 <sup>-3</sup>        | 0.10                          | 0.054    | 0.364    | -0.317    |
| Left putamen volume            | 5.63 (0.81)    | 5.79 (0.70)   | 5.56 (0.83)    | 4.40                      | 1.3 × 10 <sup>-2</sup>         | 0.56                           | 1.6 × 10 <sup>-2</sup>        | 0.35                          | 0.094    | 0.300    | -0.202    |
| Right putamen volume           | 5.55 (0.65)    | 5.69 (0.76)   | 5.41 (0.79)    | 9.49                      | <b>8.5 × 10<sup>-5*</sup></b>  | <b>2.7 × 10<sup>-2*</sup></b>  | <b>5.7 × 10<sup>-4*</sup></b> | 0.34                          | 0.191    | 0.353    | -0.190    |
| Left pallidum volume           | 1.59 (0.29)    | 1.59 (0.21)   | 1.44 (0.25)    | 32.92                     | <b>1.9 × 10<sup>-14*</sup></b> | <b>1.5 × 10<sup>-11*</sup></b> | <b>4.7 × 10<sup>-6*</sup></b> | 1.0                           | 0.559    | 0.632    | 0.013     |
| Right pallidum volume          | 1.55 (0.23)    | 1.52 (0.19)   | 1.47 (0.23)    | 10.35                     | <b>3.7 × 10<sup>-5*</sup></b>  | <b>4.5 × 10<sup>-5*</sup></b>  | 0.22                          | 0.73                          | 0.337    | 0.224    | 0.138     |
| Left hippocampus volume        | 3.91 (0.52)    | 4.02 (0.43)   | 4.17 (0.43)    | 28.91                     | <b>7.6 × 10<sup>-13*</sup></b> | <b>3.8 × 10<sup>-12*</sup></b> | <b>4.6 × 10<sup>-3*</sup></b> | 0.24                          | -0.563   | -0.346   | -0.249    |
| Right hippocampus volume       | 4.03 (0.52)    | 4.17 (0.48)   | 4.28 (0.45)    | 24.95                     | <b>3.1 × 10<sup>-11*</sup></b> | <b>5.9 × 10<sup>-11*</sup></b> | <b>2.6 × 10<sup>-2*</sup></b> | 0.14                          | -0.501   | -0.228   | -0.277    |
| Left amygdala volume           | 1.36 (0.22)    | 1.43 (0.21)   | 1.42 (0.22)    | 7.40                      | 6.6 × 10 <sup>-4</sup>         | 3.9 × 10 <sup>-4</sup>         | 1.0                           | 0.13                          | -0.277   | 0.025    | -0.309    |
| Right amygdala volume          | 1.42 (0.23)    | 1.47 (0.25)   | 1.49 (0.24)    | 7.41                      | 6.5 × 10 <sup>-4</sup>         | 5.7 × 10 <sup>-4</sup>         | 0.60                          | 0.60                          | -0.300   | -0.075   | -0.218    |
| Left accumbens volume          | 0.56 (0.15)    | 0.59 (0.16)   | 0.59 (0.16)    | 5.54                      | 4.1 × 10 <sup>-3</sup>         | 2.9 × 10 <sup>-3</sup>         | 1.0                           | 0.13                          | -0.213   | 0.0002   | -0.213    |
| Right accumbens volume         | 0.53 (0.13)    | 0.56 (0.14)   | 0.57 (0.13)    | 6.06                      | 2.4 × 10 <sup>-3</sup>         | 1.6 × 10 <sup>-3</sup>         | 1.0                           | 0.19                          | -0.255   | -0.058   | -0.187    |

The mean (SD) differences in subcortical brain volumes (cm<sup>3</sup>) among individuals with SCZ who have D-IQ or P-IQ and HC. All values, except for ICV, were analyzed with age, sex, ICV, and types of MRI machine as covariates (ICV was analyzed with age, sex, and MRI machine as covariates).

<sup>†</sup> ANCOVA.

\* $P < 5.3 \times 10^{-4}$  was considered significant.

<sup>‡</sup> Post-hoc comparisons were performed after ANCOVA using a Bonferroni correction. When there were significant differences among the groups.

\* $P < 0.05$  was considered significant. The Cohen's *d* effect sizes (*d*) are indicated. Significant differences are shown in bold.

D-IQ, deteriorated IQ; HC, healthy controls; ICV, intracranial volume; P-IQ, preserved IQ; SCZ, schizophrenia.

**Table 5.** Cortical brain volume comparisons with significant alterations in either hemisphere

| Regions                            | SCZ             |                 |                 | Statistics                |                               |                               |                               |                               | Effect size |          |           |
|------------------------------------|-----------------|-----------------|-----------------|---------------------------|-------------------------------|-------------------------------|-------------------------------|-------------------------------|-------------|----------|-----------|
|                                    | D-IQ            | P-IQ            | HC              | D-IQ–P-IQ–HC <sup>†</sup> |                               | D-IQ–HC <sup>‡</sup>          | P-IQ–HC <sup>‡</sup>          | D-IQ–P-IQ <sup>‡</sup>        | D-IQ–HC     | P-IQ–HC  | D-IQ–P-IQ |
|                                    | <i>n</i> = 111  | <i>n</i> = 54   | <i>n</i> = 633  | <i>F</i> -value           | <i>P</i> -value               | <i>P</i> -value               | <i>P</i> -value               |                               |             | <i>d</i> |           |
| Left fusiform gyrus                | 8.04<br>(1.24)  | 8.39<br>(1.29)  | 8.64<br>(1.47)  | 18.52                     | <b>1.4 × 10<sup>-8*</sup></b> | <b>1.0 × 10<sup>-8*</sup></b> | 0.22                          | 9.0 × 10 <sup>-2</sup>        | -0.438      | -0.180   | -0.274    |
| Right fusiform gyrus               | 7.77<br>(1.41)  | 8.21<br>(1.40)  | 8.25<br>(1.52)  | 12.88                     | <b>3.0 × 10<sup>-6*</sup></b> | <b>1.5 × 10<sup>-6*</sup></b> | 1.0                           | <b>1.4 × 10<sup>-2*</sup></b> | -0.322      | -0.024   | -0.310    |
| Left inferior parietal lobule      | 11.06<br>(1.61) | 11.38<br>(1.69) | 11.53<br>(1.82) | 6.96                      | 1.0 × 10 <sup>-3</sup>        | 7.5 × 10 <sup>-4</sup>        | 0.92                          | 0.48                          | -0.275      | -0.088   | -0.192    |
| Right inferior parietal lobule     | 12.51<br>(1.98) | 12.88<br>(1.96) | 13.11<br>(2.15) | 9.53                      | <b>8.1 × 10<sup>-5*</sup></b> | <b>6.6 × 10<sup>-5*</sup></b> | 0.51                          | 0.43                          | -0.289      | -0.111   | -0.187    |
| Left inferior temporal gyrus       | 8.74<br>(1.65)  | 8.86<br>(1.74)  | 9.03<br>(1.63)  | 3.50                      | 3.1 × 10 <sup>-2</sup>        | 4.2 × 10 <sup>-2</sup>        | 0.66                          | 1.0                           | -0.178      | -0.100   | -0.073    |
| Right inferior temporal gyrus      | 8.13<br>(1.63)  | 8.39<br>(1.63)  | 8.57<br>(1.61)  | 9.01                      | <b>1.4 × 10<sup>-4*</sup></b> | <b>1.3 × 10<sup>-4*</sup></b> | 0.41                          | 0.61                          | -0.275      | -0.110   | -0.163    |
| Left lateral orbitofrontal cortex  | 6.18<br>(1.02)  | 6.35<br>(0.90)  | 6.40<br>(1.16)  | 6.52                      | 1.6 × 10 <sup>-3</sup>        | 1.1 × 10 <sup>-3</sup>        | 1.0                           | 0.40                          | -0.196      | -0.046   | -0.172    |
| Right lateral orbitofrontal cortex | 6.26<br>(0.91)  | 6.38<br>(0.76)  | 6.50<br>(1.08)  | 8.18                      | <b>3.1 × 10<sup>-4*</sup></b> | <b>3.9 × 10<sup>-4*</sup></b> | 0.28                          | 1.0                           | -0.242      | -0.128   | -0.145    |
| Left lingual gyrus                 | 5.60<br>(0.97)  | 5.83<br>(1.01)  | 5.95<br>(0.93)  | 9.49                      | <b>8.4 × 10<sup>-5*</sup></b> | <b>5.6 × 10<sup>-5*</sup></b> | 0.76                          | 0.27                          | -0.369      | -0.119   | -0.237    |
| Right lingual gyrus                | 5.86<br>(0.84)  | 6.02<br>(0.93)  | 6.20<br>(0.95)  | 9.58                      | <b>7.8 × 10<sup>-5*</sup></b> | <b>9.9 × 10<sup>-5*</sup></b> | 0.24                          | 0.83                          | -0.376      | -0.191   | -0.178    |
| Left medial orbitofrontal cortex   | 4.62<br>(0.68)  | 4.60<br>(0.62)  | 4.76<br>(0.69)  | 5.70                      | 3.5 × 10 <sup>-3</sup>        | 4.6 × 10 <sup>-2</sup>        | 2.8 × 10 <sup>-2</sup>        | 1.0                           | -0.210      | -0.257   | 0.037     |
| Right medial orbitofrontal cortex  | 4.35<br>(0.60)  | 4.51<br>(0.56)  | 4.56<br>(0.65)  | 9.64                      | <b>7.3 × 10<sup>-5*</sup></b> | <b>4.4 × 10<sup>-5*</sup></b> | 0.98                          | 0.19                          | -0.339      | -0.090   | -0.271    |
| Left middle temporal gyrus         | 8.48<br>(1.47)  | 8.48<br>(1.48)  | 8.73<br>(1.53)  | 4.73                      | 9.1 × 10 <sup>-3</sup>        | 4.4 × 10 <sup>-2</sup>        | 0.10                          | 1.0                           | -0.166      | -0.168   | 0.002     |
| Right middle temporal gyrus        | 9.22<br>(1.55)  | 9.45<br>(1.59)  | 9.65<br>(1.71)  | 10.77                     | <b>2.4 × 10<sup>-5*</sup></b> | <b>3.0 × 10<sup>-5*</sup></b> | 0.21                          | 0.69                          | -0.264      | -0.123   | -0.145    |
| Left parahippocampal gyrus         | 1.66<br>(0.31)  | 1.73<br>(0.28)  | 1.79<br>(0.34)  | 13.37                     | <b>1.9 × 10<sup>-6*</sup></b> | <b>1.8 × 10<sup>-6*</sup></b> | 0.26                          | 0.30                          | -0.399      | -0.196   | -0.232    |
| Right parahippocampal gyrus        | 1.59<br>(0.32)  | 1.64<br>(0.30)  | 1.68<br>(0.33)  | 8.48                      | <b>2.3 × 10<sup>-4*</sup></b> | <b>2.2 × 10<sup>-4*</sup></b> | 0.42                          | 0.68                          | -0.286      | -0.138   | -0.158    |
| Left pars orbitalis gyrus          | 1.49<br>(0.27)  | 1.57<br>(0.30)  | 1.59<br>(0.33)  | 10.92                     | <b>2.1 × 10<sup>-5*</sup></b> | <b>1.0 × 10<sup>-5*</sup></b> | 1.0                           | <b>4.1 × 10<sup>-2*</sup></b> | -0.333      | -0.044   | -0.303    |
| Right pars orbitalis gyrus         | 1.87<br>(0.35)  | 1.90<br>(0.31)  | 1.97<br>(0.41)  | 7.36                      | 6.8 × 10 <sup>-4</sup>        | 1.4 × 10 <sup>-3</sup>        | 0.17                          | 1.0                           | -0.258      | -0.190   | -0.091    |
| Left pars triangularis             | 2.93<br>(0.48)  | 3.02<br>(0.49)  | 3.12<br>(0.63)  | 9.62                      | <b>7.5 × 10<sup>-5*</sup></b> | <b>9.1 × 10<sup>-5*</sup></b> | 0.25                          | 0.79                          | -0.342      | -0.182   | -0.184    |
| Right pars triangularis            | 3.46<br>(0.64)  | 3.72<br>(0.72)  | 3.73<br>(0.72)  | 12.86                     | <b>3.2 × 10<sup>-6*</sup></b> | <b>1.5 × 10<sup>-6*</sup></b> | 1.0                           | <b>1.2 × 10<sup>-2*</sup></b> | -0.398      | -0.016   | -0.380    |
| Left precentral gyrus              | 11.64<br>(1.38) | 11.67<br>(1.28) | 12.07<br>(1.56) | 11.28                     | <b>1.5 × 10<sup>-5*</sup></b> | <b>2.8 × 10<sup>-4*</sup></b> | <b>6.2 × 10<sup>-3*</sup></b> | 1.0                           | -0.292      | -0.280   | -0.024    |
| Right precentral gyrus             | 11.43<br>(1.39) | 11.71<br>(1.42) | 11.89<br>(1.63) | 7.59                      | 5.5 × 10 <sup>-4</sup>        | 5.2 × 10 <sup>-4</sup>        | 0.51                          | 0.73                          | -0.303      | -0.119   | -0.198    |
| Left rostral middle frontal gyrus  | 12.70<br>(1.96) | 12.80<br>(2.15) | 13.10<br>(2.29) | 6.99                      | 9.8 × 10 <sup>-4</sup>        | 3.0 × 10 <sup>-3</sup>        | 0.11                          | 1.0                           | -0.204      | -0.146   | -0.054    |
|                                    | 12.80<br>(2.08) | 12.90<br>(2.09) | 13.50<br>(2.47) | 15.82                     | <b>1.8 × 10<sup>-7*</sup></b> | <b>4.0 × 10<sup>-6*</sup></b> | <b>2.7 × 10<sup>-3*</sup></b> | 1.0                           | -0.297      | -0.252   | -0.048    |

**Table 5.** (Continued)

| Regions                            | SCZ             |                 |                 | Statistics                |                                |                               |                               |                               | Effect size |         |           |
|------------------------------------|-----------------|-----------------|-----------------|---------------------------|--------------------------------|-------------------------------|-------------------------------|-------------------------------|-------------|---------|-----------|
|                                    | D-IQ            | P-IQ            | HC              | D-IQ–P-IQ–HC <sup>†</sup> |                                | D-IQ–HC <sup>‡</sup>          | P-IQ–HC <sup>‡</sup>          | D-IQ–P-IQ <sup>‡</sup>        | D-IQ–HC     | P-IQ–HC | D-IQ–P-IQ |
|                                    | <i>n</i> = 111  | <i>n</i> = 54   | <i>n</i> = 633  | <i>F</i> -value           | <i>P</i> -value                | <i>P</i> -value               |                               |                               | <i>d</i>    |         |           |
| Right rostral middle frontal gyrus |                 |                 |                 |                           |                                |                               |                               |                               |             |         |           |
| Left superior frontal gyrus        | 18.00<br>(2.39) | 18.20<br>(2.41) | 19.00<br>(2.72) | 24.91                     | <b>3.2 × 10<sup>-11*</sup></b> | <b>1.1 × 10<sup>-9*</sup></b> | <b>5.3 × 10<sup>-4*</sup></b> | 1.0                           | -0.391      | -0.310  | -0.086    |
| Right superior frontal gyrus       | 17.20<br>(2.17) | 17.20<br>(2.26) | 18.10<br>(2.76) | 25.19                     | <b>2.5 × 10<sup>-11*</sup></b> | <b>6.2 × 10<sup>-9*</sup></b> | <b>4.9 × 10<sup>-5*</sup></b> | 1.0                           | -0.387      | -0.363  | -0.021    |
| Left superior temporal gyrus       | 9.52<br>(1.47)  | 10.10<br>(1.45) | 10.10<br>(1.71) | 13.54                     | <b>1.7 × 10<sup>-6*</sup></b>  | <b>7.9 × 10<sup>-7*</sup></b> | 1.0                           | <b>7.8 × 10<sup>-3*</sup></b> | -0.355      | 0.004   | -0.391    |
| Right superior temporal gyrus      | 9.36<br>(1.41)  | 9.67<br>(1.27)  | 9.84<br>(1.65)  | 11.58                     | <b>1.1 × 10<sup>-5*</sup></b>  | <b>7.8 × 10<sup>-6*</sup></b> | 0.50                          | 0.24                          | -0.314      | -0.117  | -0.232    |
| Left insula                        | 6.26<br>(0.87)  | 6.58<br>(0.87)  | 6.46<br>(0.96)  | 7.97                      | <b>3.7 × 10<sup>-4*</sup></b>  | <b>7.5 × 10<sup>-4*</sup></b> | 0.77                          | <b>3.5 × 10<sup>-3*</sup></b> | -0.218      | 0.128   | -0.364    |
| Right insula                       | 6.60<br>(0.99)  | 6.62<br>(0.91)  | 6.68<br>(1.04)  | 1.39                      | 0.25                           | 0.69                          | 0.60                          | 1.0                           | -0.080      | -0.064  | -0.019    |

The mean (SD) differences in cortical brain volumes (cm<sup>3</sup>) with significant alterations in either hemisphere among individuals with SCZ who have D-IQ or P-IQ and HC. Covariates appearing in the model were age, sex, intracranial volume, and type of MRI scanner.  
<sup>\*</sup>*P* < 5.3 × 10<sup>-4</sup> was considered significant.  
<sup>†</sup>Post-hoc comparisons were performed after ANCOVA using a Bonferroni correction. When there were significant differences among the groups.  
<sup>\*</sup>*P* < 0.05 was considered significant. The Cohen's *d* effect sizes (*d*) are indicated. Significant differences are shown in bold.  
 D-IQ, deteriorated IQ; HC, healthy controls; P-IQ, preserved IQ; SCZ, schizophrenia.

groups; however, there was no significant difference between the preserved and deteriorated groups (Table 1). The HC group had a higher current IQ score than the preserved and deteriorated groups, and the

preserved group had a higher current IQ score than the deteriorated group, as defined in this study (Table 1). Similar to the current IQ score, memory performance data also showed lower memory

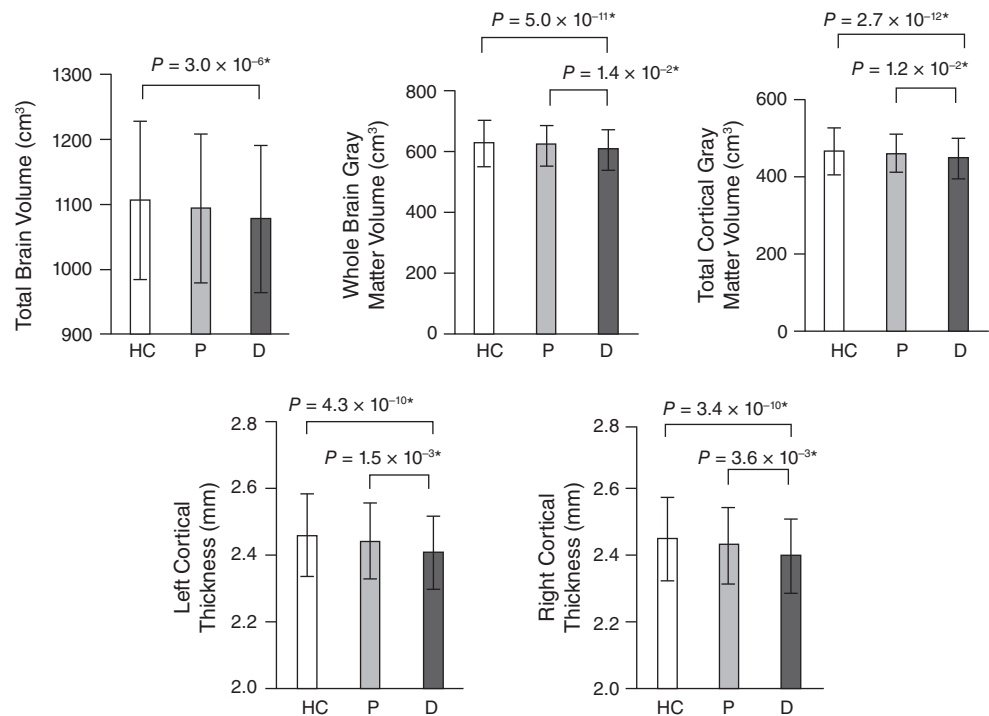


**Fig. 1** Volume differences in brain structures among groups. The mean differences in brain structures across healthy controls (HC) and individuals with schizophrenia who show preserved IQ (P) or deteriorated IQ (D). Error bars are the standard deviation of the mean (SD). Statistical significance was defined for post-hoc comparisons at *P* < 0.05.

performance in the two schizophrenia groups than in the HC group, and memory performance was much lower in the deteriorated group than in the preserved group (Table 1).

We compared clinical data between the deteriorated and preserved groups. No significant differences in age of onset or periods of illness were observed between the two groups (Table 2). However, the Global Assessment of Functioning score was significantly higher in the preserved group than in the deteriorated group. The PANSS total score, Negative score, and General score were significantly better in the preserved group than in the deteriorated group, while the PANSS Positive score was not significantly different between the two schizophrenia groups (Table 2). Daily doses of antipsychotics, based on the total amount of chlorpromazine equivalence (CPZeq), and CPZeq of typical antipsychotic drugs in the deteriorated group were significantly higher than those in the preserved group (Table 2). These data suggested that the deteriorated group had more severe clinical symptoms and was administered more antipsychotic drugs than the preserved group.

### Structural imaging analysis

The deteriorated group showed more extensive abnormal brain structures than the HC, and this effect was not apparent in the preserved group (Tables 3–5, Figs 1,2). The deteriorated group showed significantly decreased whole brain gray matter and total cortical gray matter volumes and decreased bilateral cortical thickness (Table 3, Fig. 1); increased right lateral ventricle volume (Table 4); and decreased volumes of the right fusiform gyrus, left pars orbitalis gyrus, right pars triangularis, left superior temporal gyrus, and left insula (Tables 5 and S1), compared to those in the HC group and in the preserved group, while there were no significant differences in these areas between the preserved and HC groups. These results might suggest that alterations in these brain areas were specific morphological features in the deteriorated subgroup of schizophrenia. Compared to the HC group, the deteriorated group showed

significantly decreased total brain volume (Table 3, Fig. 1), increased right pallidum volume (Table 4, Fig. 2), and decreased volumes of the left fusiform gyrus, right inferior parietal lobule, right inferior temporal gyrus, right lateral orbitofrontal cortex, bilateral lingual gyrus, right medial orbitofrontal cortex, right middle temporal gyrus, bilateral parahippocampal gyrus, left pars triangularis, and right superior temporal gyrus (Table 5), while there were no significant differences in these measures between the preserved group and the other two groups (Tables 3–5 and S1, Figs 1,2).

Compared to the HC group, both the deteriorated and preserved groups showed significantly increased volumes in the left lateral ventricle, right putamen, and left pallidum, a decreased bilateral hippocampal volume (Table 4, Fig. 2), and decreased volumes of the left precentral gyrus, right rostral middle frontal gyrus, and bilateral superior frontal gyrus (Table 5); however, no significant differences in the volumes of these regions were observed between the deteriorated and preserved groups (Tables 4,5 and S1, Fig. 2). These results suggested that these morphological brain alterations appeared in schizophrenia regardless of the cognitive subgroup. The cortical brain volumes for all regions are shown in Table S1. In addition, correlational analysis between the 94 brain morphological values and the degree of cognitive decline in patients with schizophrenia did not show any significant correlation, except for left cortical thickness ( $P = 2.19 \times 10^{-4}$ ).

### Brain connectivity analysis

To examine the influence of the alterations in subcortical and cortical volumes in brain physiology, we analyzed brain connectivity between subcortical regions, such as the thalamus, accumbens, amygdala, caudate nucleus, hippocampus, pallidum, and putamen as seeds and other brain regions using a subset of subjects from the structural analysis (deteriorated patients,  $n = 40$ ; preserved patients,  $n = 20$ ; HC,  $n = 234$ ; detailed information in Table S2).

We compared functional connectivity maps seeded in the bilateral thalamus between the two cognitive phenotype groups and the HC group

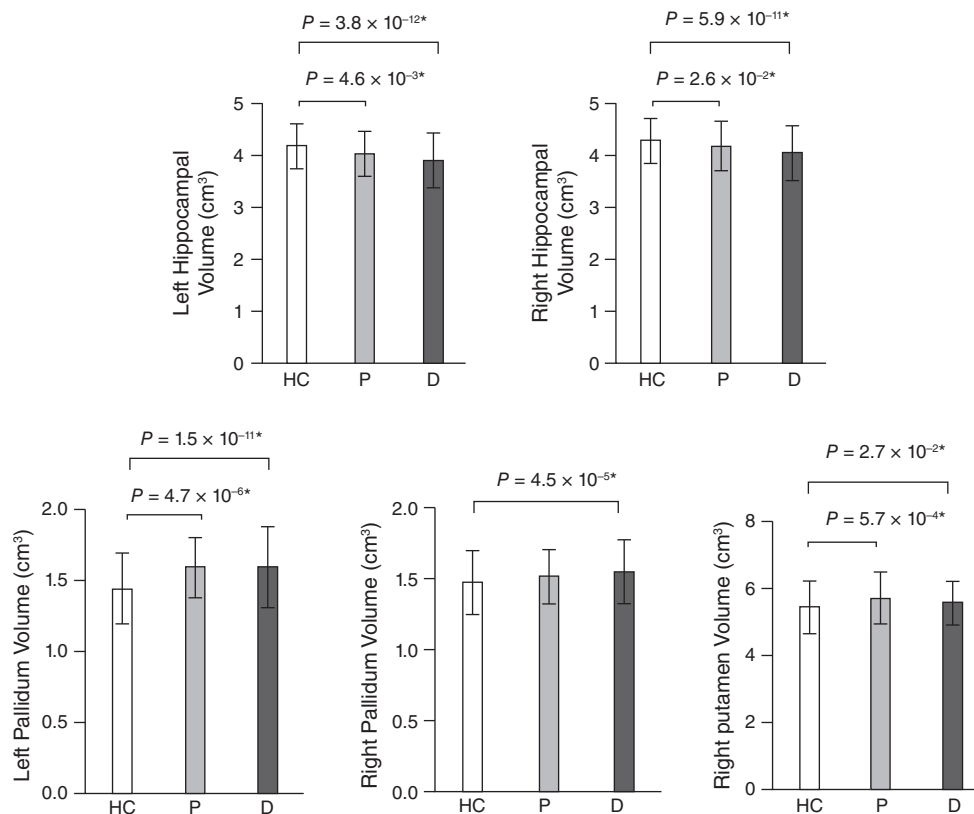


**Fig.2** Volume differences in subcortical brain structures among groups. The mean differences in subcortical brain volume across healthy controls (HC) and individuals with schizophrenia who show preserved IQ (P) or deteriorated IQ (D). Error bars are the standard deviation of the mean (SD). Statistical significance was defined for post-hoc comparisons at  $P < 0.05$ .

**Table 6.** Hyperconnectivity between the thalamus and other brain regions in D-IQ and P-IQ schizophrenia patients

|   | Region                    | Left thalamus (seed) |            | Right thalamus (seed) |      |
|---|---------------------------|----------------------|------------|-----------------------|------|
|   |                           | D-IQ                 | P-IQ       | D-IQ                  | P-IQ |
| Hyperconnectivity in D-IQ and P-IQ patients | Cingulate gyrus           | Left/right           | Left/right |                       |      |
|   | Fusiform gyrus            |                      |            | Left                  | Left |
|   | Inferior frontal gyrus    |                      |            | Left                  | Left |
|   | Inferior parietal lobule  | Left/right           | Left/right | Left                  | Left |
|   | Inferior temporal gyrus   |                      |            | Left                  | Left |
|   | Medial frontal gyrus      | Left/right           | Left/right | Left                  | Left |
|   | Middle frontal gyrus      | Left/right           | Left/right | Left                  | Left |
|   | Middle temporal gyrus     | Right                | Right      | Left                  | Left |
|   | Paracentral lobule        | Left/right           | Left/right |                       |      |
|   | Postcentral gyrus         | Left/right           | Left/right | Left                  | Left |
|   | Precentral gyrus          | Left/right           | Left/right | Left                  | Left |
|   | Precuneus                 | Left/right           | Left/right |                       |      |
|   | Superior frontal gyrus    | Left                 | Left       | Left                  | Left |
|   | Superior parietal lobule  | Left                 | Left       |                       |      |
| Superior temporal gyrus                     | Right                     | Right                |            |                       |      |
| Hyperconnectivity only in D-IQ patients     | Angular gyrus             | Left/right           |            | Left/right            |      |
|   | Anterior cingulate        | Left/right           |            | Left/right            |      |
|   | Caudate                   | Left/right           |            | Left/right            |      |
|   | Cingulate gyrus           |                      |            | Left/right            |      |
|   | Clastrum                  | Left/right           |            | Left/right            |      |
|   | Cuneus                    | Left/right           |            | Left/right            |      |
|   | Fusiform gyrus            | Left/right           |            | Right                 |      |
|   | Inferior frontal gyrus    | Left/right           |            | Right                 |      |
|   | Inferior occipital gyrus  | Left/right           |            | Left/right            |      |
|   | Inferior parietal lobule  |                      |            | Right                 |      |
|   | Inferior temporal gyrus   | Left/right           |            | Right                 |      |
|   | Insula                    | Left/right           |            | Left/right            |      |
|   | Lentiform nucleus         | Left/right           |            | Left/right            |      |
|   | Lingual gyrus             | Left/right           |            | Left/right            |      |
|   | Medial frontal gyrus      |                      |            | Right                 |      |
|   | Middle frontal gyrus      |                      |            | Right                 |      |
|   | Middle occipital gyrus    | Left/right           |            | Left/right            |      |
|   | Middle temporal gyrus     | Left                 |            | Right                 |      |
|   | Paracentral lobule        |                      |            | Left/right            |      |
|   | Parahippocampal gyrus     | Left/right           |            | Left/right            |      |
|   | Postcentral gyrus         |                      |            | Right                 |      |
|   | Posterior cingulate       | Left/right           |            | Left/right            |      |
|   | Precentral gyrus          |                      |            | Right                 |      |
|   | Precuneus                 |                      |            | Left/right            |      |
|   | Subcallosal gyrus         | Right                |            | Right                 |      |
|   | Superior frontal gyrus    | Right                |            | Right                 |      |
|   | Superior occipital gyrus  | Left/right           |            | Left/right            |      |
|   | Superior parietal lobule  | Right                |            | Left/right            |      |
|   | Superior temporal gyrus   | Left                 |            | Left/right            |      |
|   | Supramarginal gyrus       | Left/right           |            | Left/right            |      |
|   | Transverse temporal gyrus | Left/right           |            | Left/right            |      |
|   | Uncus                     | Left/right           |            | Left/right            |      |

Brain regions are shown that exhibited significant connectivity with the left or right thalamus when they were used as the seeds in patients with schizophrenia with D-IQ or P-IQ compared with connectivity in healthy controls. The threshold for significance was set at a cluster-level family-wise-error-corrected  $P < 0.05$ .

D-IQ, deteriorated IQ; P-IQ, preserved IQ.

(Table 6, Fig. 3). Hyperconnectivity between the thalamus and widespread cortical areas was observed in the deteriorated group compared with connectivity between these regions in HC. Most of the regions

showing hyperconnectivity with the thalamus were found only in deteriorated patients, and this hyperconnectivity was not prominent in the frontal lobe (Fig. 3). However, hyperconnectivity in several cortical regions,

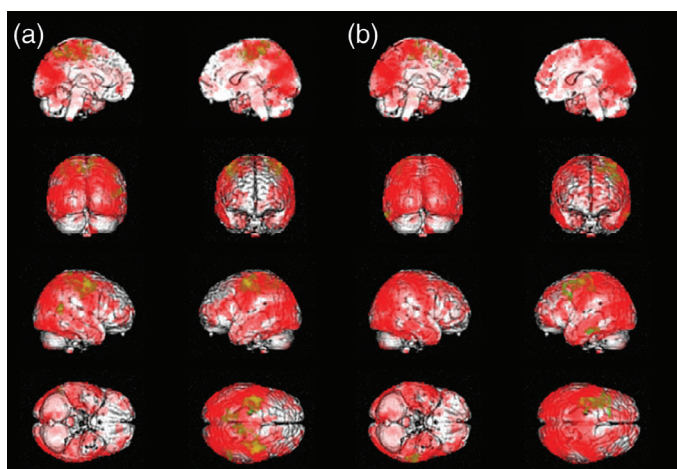


**Fig.3** Hyperconnectivity between the thalamus and widespread cortical areas in deteriorated patients. Hyperconnectivity between the (a) left thalamus and (b) right thalamus and other brain areas are shown. Red indicates significant hyperconnectivity in the deteriorated patients compared with connectivity in healthy controls (HC), green indicates significant hyperconnectivity in the preserved group compared with connectivity in HC, and yellow indicates merged areas of red and green. The threshold for significance was set at a cluster-level family-wise-error-corrected  $P < 0.05$ .

including the inferior parietal lobule, medial frontal gyrus, middle frontal gyrus, middle temporal gyrus, postcentral gyrus, precentral gyrus, and superior frontal gyrus, was observed in both deteriorated and preserved patients. Hypoconnectivity between the bilateral thalamus and contralateral thalamus was found only in deteriorated patients compared with the connectivity between these regions in HC (data not shown). No brain regions had significantly different levels of connectivity between the two schizophrenia cognitive subgroups (data not shown).

We compared functional connectivity maps seeded in the bilateral accumbens and other subcortical regions among the two cognitive phenotype groups and the HC group. Overall, hyperconnectivity between seeds of subcortical regions and other subcortical regions, the posterior cingulate, precuneus, and cuneus was prominent in deteriorated patients compared with the connectivity between these regions in HC, while hyperconnectivity in these regions was not apparent in preserved patients compared with connectivity in HC (Table S3, Figs S2–S9). However, hyperconnectivity between the accumbens seed and the frontal, temporal, and precentral gyri was observed in preserved patients compared with HC; while, hyperconnectivity between the accumbens seed and abovementioned cortical areas was not observed in deteriorated patients compared with connectivity in HC (Fig. 4a,b, Table S3). A direct comparison of the functional connectivity between preserved and deteriorated patients

revealed that preserved patients showed significant hyperconnectivity between the accumbens seed and the superior and middle frontal gyri (Fig. 4c, Table S3). No brain regions showed significant hyperconnectivity with any seed region, except the accumbens, in the two schizophrenia cognitive subgroups (data not shown).

Hypoconnectivity between seeds in the amygdala, hippocampus, pallidum and putamen, and cortical areas, including the insula, temporal gyrus, frontal gyrus, central gyrus, and cingulate gyrus, was observed in deteriorated patients compared with connectivity in HC, and similar, but less prominent, hypoconnectivity between seeds in the putamen was observed in preserved patients compared with connectivity of HC (Table S4 and Figs S10–S14). No brain regions showed significant hypoconnectivity with any seed region between the two schizophrenia cognitive subgroups (data not shown).

Correlational analysis between cognitive decline in patients and functional connectivity with all subcortical regions as seeds was performed. No correlation was observed except for the positive correlation between the seed in the left hippocampus and the right insula and transverse temporal gyrus (Table S5 and Fig. S15).

## Discussion

In this study, we revealed that the deteriorated patients with schizophrenia had a broader range of changes in brain structures and functional connectivity than the preserved patients with schizophrenia. We confirmed increased left lateral ventricle and left pallidum volume and decreased bilateral hippocampus, left precentral gyrus, right rostral middle frontal gyrus, and bilateral superior frontal gyrus volume in deteriorated and preserved patients compared to controls in a cohort with a larger sample size than that in previous studies,<sup>23,24</sup> suggesting that these brain structural alterations in schizophrenia were not specific to cognitive subgroups. We also revealed that reductions in whole brain gray matter, total cortical gray matter, right lateral ventricle, right fusiform gyrus, left pars orbitalis gyrus, right pars triangularis, left superior temporal gyrus and left insula volumes, and bilateral cortical thickness were characteristic brain structural alterations in the deteriorated cognitive subgroup. Previous studies have reported that high-risk individuals show hippocampal and amygdalar abnormalities before schizophrenia onset.<sup>35,36</sup> The right pars triangularis was reported to be smaller in individuals at high risk for schizophrenia or schizoaffective disorder than in controls.<sup>37,38</sup> These reports and our findings suggest that high-risk individuals with a smaller right pars triangularis gyrus volume may be more likely to develop a deteriorated cognitive profile in schizophrenia.

Brain functional connectivity analysis showed abnormal connectivity, such as hyperconnectivity, between the thalamus and cortical regions, which was a dominant pattern in deteriorated patients with schizophrenia, suggesting that these alterations could be related to the neurophysiological mechanisms of cognitive impairment in schizophrenia. We found hyperconnectivity between the thalamus and a broad range of brain regions in the deteriorated patients with

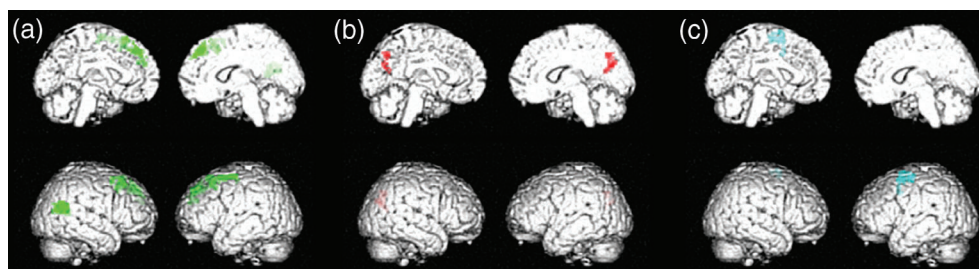


**Fig.4** Hyperconnectivity between the accumbens and the frontal and temporal gyri in preserved patients. Hyperconnectivity between the right accumbens and other brain areas in preserved patients compared with connectivity in (a) healthy controls (HC), (b) deteriorated patients compared with that in HC, and (c) preserved patients compared with that in deteriorated patients are shown. Green indicates significant hyperconnectivity in the preserved patients compared with connectivity in HC. Red indicates significant hyperconnectivity in the deteriorated patients compared with connectivity in HC. Light blue indicates significant hyperconnectivity in the preserved patients compared with connectivity in deteriorated patients. The threshold for significance was set at a cluster-level family-wise-error-corrected  $P < 0.05$ .

schizophrenia, but this effect was not prominent in the frontal lobe (Fig. 3, Table 6). Hyperconnectivity between the thalamus and brain regions in preserved patients with schizophrenia was much less evident than that in deteriorated patients with schizophrenia. Prior rsfMRI studies in patients with schizophrenia have reported decreased thalamo-prefrontal connectivity and increased thalamotemporal and thalamo-sensorimotor connectivity.<sup>39,40</sup> The thalamus is known for relaying sensory and motor signals to cortical regions, a function that could underlie the neurobiology of sensorimotor gating abnormalities observed in patients with schizophrenia.<sup>41</sup> An experimental animal study reported auditory sensory gating functions in reticular thalamic neurons, which were disrupted by the psychostimulant D-amphetamine.<sup>42</sup> Taken together, thalamotemporal and thalamo-sensorimotor hyperconnectivity could be a physiological biomarker of cognitive dysfunction in schizophrenia related to abnormal sensorimotor gating.

Hyperconnectivity between the accumbens and superior/middle frontal gyrus was observed in preserved patients compared with the connectivity in deteriorated patients (Fig. 4 and Table S3). One of the dopaminergic pathways, the mesocorticolimbic pathway, functions as a reward system that controls the response to rewards. The nucleus accumbens and the frontal gyrus are included in the mesocorticolimbic pathway, and the accumbens play an important role in the reward system. Because intrinsic motivation is impaired in patients with schizophrenia, it is essential to enhance intrinsic motivation during cognitive remediation therapies, which is one of the most effective cognition-enhancing methods in schizophrenia.<sup>43</sup> Taken together, hyperconnectivity between the accumbens and the frontal gyrus in preserved patients might be related to protective alterations in preserved patients.

Hyperconnectivity among the subcortical regions, including the amygdala-caudate, pallidum-caudate, and pallidum-thalamus connections, was observed in deteriorated patients with schizophrenia (Table S3). There are anatomical projections from the amygdala to the caudate, from the caudate to the pallidum, and from the pallidum to the thalamus, and this circuit is involved in emotional behaviors. As more negative symptoms were observed in the deteriorated patients with schizophrenia than in the preserved patients, the hyperconnectivity of this circuit might be a compensatory alteration.

Hypoconnectivity between subcortical regions and the insula and cingulate gyrus was prominent in deteriorated patients with schizophrenia; however, this hypoconnectivity was much less evident in preserved patients (Table S4). The insula and cingulate gyrus have been implicated in cognitive, affective, and regulatory functions, and these regions form a salience network that functions to emphasize the most relevant of all internal and external stimuli to guide behavior. The salience network plays a crucial role in the dynamic switching between endogenously mediated/self-referential mental activity (default mode network) and exogenously driven/cognitively demanding mental activity (central executive network).<sup>34</sup> Because salience network dysfunction has been demonstrated in schizophrenia and might be related to cognitive impairment in schizophrenia,<sup>45</sup> this dysfunction could be due to the hypoconnectivity between subcortical regions and the insula and cingulate gyrus, which are important components of the salience network.

Our study has several limitations. First, the estimated premorbid IQ score was retrospectively calculated. Second, it is possible that the disease may progress in preserved patients with schizophrenia, meaning that later these patients could be categorized into the deteriorated patients with schizophrenia subgroup. In this case, the differential alterations in brain structure and functional connectivity among the cognitive subgroups would have only reflected a particular stage of the disease. However, there was no significant difference in either the age of onset or the duration of the illness between the deteriorated and preserved patients. These results support the notion that the preserved patients could not be an earlier stage of the disease than deteriorated patients. Third, the structural and functional brain alterations between the two cognitive subgroups could not be due to the subgroups but only to the degree of cognitive decline. The correlational

analysis between the brain phenotypes and degree of cognitive decline showed little evidence for an association (left thickness and connectivity between left hippocampus and right insula and transverse temporal gyrus), suggesting that differential brain morphology and function might be influenced by cognitive subgroups rather than the degree of cognitive decline. However, further studies using a larger sample size may be useful for drawing conclusions.

In this study, we replicated altered brain structures between cognitive subgroups based on IQ decline in schizophrenia, consistent with previous findings, in a larger cohort.<sup>23,24</sup> Moreover, we observed possible hyper- and hypoconnectivities between subcortical regions and a broad range of brain regions in patients in different cognitive subgroups. These results suggest the possibility that subgroups based on levels of IQ decline may be useful for the exploration of brain pathophysiology in patients with schizophrenia. Because cognitive impairments and brain structural alterations are often found in schizophrenia but are not specific features of schizophrenia, a similar examination in other forms of psychosis is warranted for future investigation.

### Acknowledgments

We thank all participants in this study. This work was supported in part by Brain/MINDS (JP18dm0207006; JP19dm0207069), Brain/MINDS beyond (JP19dm0307002; JP19dm0307001; JP19dm0307004), and Health and Labor Sciences Research Grants for Comprehensive Research on Persons with Disabilities (16dk0307031h0003) from AMED, Grants-in-Aid for Scientific Research (KAKENHI; Grant Number: JP25293250; JP16H05375; JP16H06280; JP17H04244) and the International Research Center for Neurointelligence (WPI-IRCN) at The University of Tokyo Institutes for Advanced Study (UTIAS). The funders had no role in the study design, data collection and analysis, decision to publish, or preparation of the manuscript. Some computations were performed at the Research Center for Computational Science, Okazaki, Japan.

### Disclosure statement

All authors declare no relevant conflicts of interest in relation to the subject of this manuscript.

### Author contributions

Y.Y. was critically involved in data collection and data analysis and wrote the first draft of the manuscript. N.O., M.F., and K.N. were involved in the data analysis and contributed to the interpretation of the data and the writing of the manuscript. D.K., T.S., S.M., K.O., K.M., and K.M. were involved in the data analysis and contributed to the interpretation of the data. H.Y., N.K., H.A., M.F., and Y.W. were involved in data collection and data analysis. Y.W. and K.K. were involved in data collection and contributed to the interpretation of the data. R.H. supervised the entire project, collected the data, and was critically involved in the design, analysis, and interpretation of the data. All authors contributed to and approved the final manuscript.

### References

- Barch DM, Sheffield JM. Cognitive impairments in psychotic disorders: Common mechanisms and measurement. *World Psychiatry* 2014; **13**: 224–232.
- Schaefer J, Giangrande E, Weinberger DR, Dickinson D. The global cognitive impairment in schizophrenia: Consistent over decades and around the world. *Schizophr. Res.* 2013; **150**: 42–50.
- Tandon R, Gaebel W, Barch DM *et al.* Definition and description of schizophrenia in the DSM-5. *Schizophr. Res.* 2013; **150**: 3–10.
- Nuechterlein KH, Subotnik KL, Green MF *et al.* Neurocognitive predictors of work outcome in recent-onset schizophrenia. *Schizophr. Bull.* 2011; **37**: S33–S40.
- Fett AK, Viechtbauer W, Dominguez MD, Penn DL, van Os J, Krabbendam L. The relationship between neurocognition and social cognition with functional outcomes in schizophrenia: A meta-analysis. *Neurosci. Biobehav. Rev.* 2011; **35**: 573–588.

6. Tolman AW, Kurtz MM. Neurocognitive predictors of objective and subjective quality of life in individuals with schizophrenia: A meta-analytic investigation. *Schizophr. Bull.* 2012; **38**: 304–315.
7. Lesh TA, Niendam TA, Minzenberg MJ, Carter CS. Cognitive control deficits in schizophrenia: Mechanisms and meaning. *Neuropsychopharmacology* 2011; **36**: 316–338.
8. Fujino H, Sumiyoshi C, Sumiyoshi T *et al.* Predicting employment status and subjective quality of life in patients with schizophrenia. *Schizophr. Res. Cogn.* 2016; **3**: 20–25.
9. Sawada K, Kanehara A, Sakakibara E *et al.* Identifying neurocognitive markers for outcome prediction of global functioning in individuals with first-episode and ultra-high-risk for psychosis. *Psychiatry Clin. Neurosci.* 2017; **71**: 318–327.
10. Nakagome K. Cognitive impairment in psychiatric disorders. *Psychiatry Clin. Neurosci.* 2017; **71**: 293–293.
11. Guo X, Li J, Wang J *et al.* Hippocampal and orbital inferior frontal gray matter volume abnormalities and cognitive deficit in treatment-naive, first-episode patients with schizophrenia. *Schizophr. Res.* 2014; **152**: 339–343.
12. Herold CJ, Lasser MM, Schmid LA *et al.* Neuropsychology, autobiographical memory, and hippocampal volume in “younger” and “older” patients with chronic schizophrenia. *Front. Psych.* 2015; **6**: 53.
13. Karnik-Henry MS, Wang L, Barch DM, Harms MP, Campanella C, Csernansky JG. Medial temporal lobe structure and cognition in individuals with schizophrenia and in their non-psychotic siblings. *Schizophr. Res.* 2012; **138**: 128–135.
14. Knochel C, Stablein M, Storchak H *et al.* Multimodal assessments of the hippocampal formation in schizophrenia and bipolar disorder: Evidences from neurobehavioral measures and functional and structural MRI. *NeuroImage Clin.* 2014; **6**: 134–144.
15. Bakhshi K, Chance SA. The neuropathology of schizophrenia: A selective review of past studies and emerging themes in brain structure and cytoarchitecture. *Neuroscience* 2015; **303**: 82–102.
16. van Erp TG, Hibar DP, Rasmussen JM *et al.* Subcortical brain volume abnormalities in 2028 individuals with schizophrenia and 2540 healthy controls via the ENIGMA consortium. *Mol. Psychiatry* 2016; **21**: 547–553.
17. Okada N, Fukunaga M, Yamashita F *et al.* Abnormal asymmetries in subcortical brain volume in schizophrenia. *Mol. Psychiatry* 2016; **21**: 1460–1466.
18. Koshiyama D, Fukunaga M, Okada N *et al.* Subcortical association with memory performance in schizophrenia: A structural magnetic resonance imaging study. *Transl. Psychiatry* 2018; **8**: 20.
19. Koshiyama D, Fukunaga M, Okada N *et al.* Role of subcortical structures on cognitive and social function in schizophrenia. *Sci. Rep.* 2018; **8**: 1183.
20. Koshiyama D, Fukunaga M, Okada N *et al.* Role of frontal white matter and corpus callosum on social function in schizophrenia. *Schizophr. Res.* 2018; **202**: 180–187.
21. Ohi K, Sumiyoshi C, Fujino H *et al.* A brief assessment of intelligence decline in schizophrenia as represented by the difference between current and premorbid intellectual quotient. *Front. Psych.* 2017; **8**: 293.
22. Weickert TW, Goldberg TE, Gold JM, Bigelow LB, Egan MF, Weinberger DR. Cognitive impairments in patients with schizophrenia displaying preserved and compromised intellect. *Arch. Gen. Psychiatry* 2000; **57**: 907–913.
23. Czepielewski LS, Wang L, Gama CS, Barch DM. The relationship of intellectual functioning and cognitive performance to brain structure in schizophrenia. *Schizophr. Bull.* 2017; **43**: 355–364.
24. Weinberg D, Lenroot R, Jacomb I *et al.* Cognitive subtypes of schizophrenia characterized by differential brain volumetric reductions and cognitive decline. *JAMA Psychiatry* 2016; **73**: 1251–1259.
25. Fujino H, Sumiyoshi C, Yasuda Y *et al.* Estimated cognitive decline in patients with schizophrenia: A multicenter study. *Psychiatry Clin. Neurosci.* 2017; **71**: 294–300.
26. Wechsler D. *Administration and scoring manual for the Wechsler Adult Intelligence Scale.* Psychological Corporation, San Antonio, TX, 1997.
27. Matsuoka K, Uno M, Kasai K, Koyama K, Kim Y. Estimation of premorbid IQ in individuals with Alzheimer's disease using Japanese ideographic script (Kanji) compound words: Japanese version of National Adult Reading Test. *Psychiatry Clin. Neurosci.* 2006; **60**: 332–339.
28. Wechsler D. *Manual for the Wechsler Adult Intelligence Scale-Revised.* Psychological Corporation, New York, NY, 1987.
29. Kay SR, Fiszbein A, Opler LA. The Positive and Negative Syndrome Scale (PANSS) for schizophrenia. *Schizophr. Bull.* 1987; **13**: 261–276.
30. Fischl B. FreeSurfer. *NeuroImage* 2012; **62**: 774–781.
31. Chao-Gan Y, Yu-Feng Z. DPARSF: A MATLAB toolbox for “pipeline” data analysis of resting-state fMRI. *Front. Syst. Neurosci.* 2010; **4**: 13.
32. Yan CG, Wang XD, Zuo XN, Zang YF. DPABI: Data processing & analysis for (resting-state) brain imaging. *Neuroinformatics* 2016; **14**: 339–351.
33. Friston KJ, Williams S, Howard R, Frackowiak RS, Turner R. Movement-related effects in fMRI time-series. *Magn. Reson. Med.* 1996; **35**: 346–355.
34. Power JD, Barnes KA, Snyder AZ, Schlaggar BL, Petersen SE. Spurious but systematic correlations in functional connectivity MRI networks arise from subject motion. *NeuroImage* 2012; **59**: 2142–2154.
35. Lawrie SM, Whalley HC, Job DE, Johnstone EC. Structural and functional abnormalities of the amygdala in schizophrenia. *Ann. N. Y. Acad. Sci.* 2003; **985**: 445–460.
36. Ganzola R, Maziade M, Duchesne S. Hippocampus and amygdala volumes in children and young adults at high-risk of schizophrenia: Research synthesis. *Schizophr. Res.* 2014; **156**: 76–86.
37. Li G, Wang L, Shi F *et al.* Cortical thickness and surface area in neonates at high risk for schizophrenia. *Brain Struct. Funct.* 2016; **221**: 447–461.
38. Iwashiro N, Suga M, Takano Y *et al.* Localized gray matter volume reductions in the pars triangularis of the inferior frontal gyrus in individuals at clinical high-risk for psychosis and first episode for schizophrenia. *Schizophr. Res.* 2012; **137**: 124–131.
39. Woodward ND, Karbasforoushan H, Heckers S. Thalamocortical dysconnectivity in schizophrenia. *Am. J. Psychiatry* 2012; **169**: 1092–1099.
40. Li T, Wang Q, Zhang J *et al.* Brain-wide analysis of functional connectivity in first-episode and chronic stages of schizophrenia. *Schizophr. Bull.* 2017; **43**: 436–448.
41. Ferrarelli F, Tononi G. The thalamic reticular nucleus and schizophrenia. *Schizophr. Bull.* 2011; **37**: 306–315.
42. Krause M, Hoffmann WE, Hajos M. Auditory sensory gating in hippocampus and reticular thalamic neurons in anesthetized rats. *Biol. Psychiatry* 2003; **53**: 244–253.
43. Takeda K, Sumiyoshi T, Matsumoto M *et al.* Neural correlates for intrinsic motivational deficits of schizophrenia; implications for therapeutics of cognitive impairment. *Front. Psych.* 2018; **9**: 178.
44. Menon V, Uddin LQ. Saliency, switching, attention and control: A network model of insula function. *Brain Struct. Funct.* 2010; **214**: 655–667.
45. Palaniyappan L, White TP, Liddle PF. The concept of salience network dysfunction in schizophrenia: From neuroimaging observations to therapeutic opportunities. *Curr. Top. Med. Chem.* 2012; **12**: 2324–2338.

### Supporting information

Additional Supporting Information may be found in the online version of this article at the publisher's web-site:

**Table S1.** Comparisons of the cortical brain volume of all regions among subgroups.

**Table S2.** Basic demographic information for the subjects in the brain connectivity analysis.

**Table S3.** Hyperconnectivity between subcortical regions and other brain regions in deteriorated and preserved patients.

**Table S4.** Hypoconnectivity between subcortical regions and other brain regions in deteriorated and preserved patients.

**Table S5.** Correlation between functional connectivity and cognitive decline in patients.

**Fig. S1.** Scattergram of the difference values between current and premorbid IQ in all patients and control subjects.

**Fig. S2.** Hyperconnectivity between the accumbens and other brain regions in deteriorated patients.

**Fig. S3.** Hyperconnectivity between the amygdala and other brain regions in deteriorated patients.

**Fig. S4.** Hyperconnectivity between the caudate and other brain regions in deteriorated patients.

**Fig. S5.** Hyperconnectivity between the caudate and other brain regions in preserved patients.

**Fig. S6.** Hyperconnectivity between the hippocampus and other brain regions in deteriorated patients.

**Fig. S7.** Hyperconnectivity between the pallidum and other brain regions in deteriorated patients.

**Fig. S8.** Hyperconnectivity between the putamen and other brain regions in deteriorated patients.

**Fig. S9.** Hyperconnectivity between the putamen and other brain regions in preserved patients.

**Fig. S10.** Hypoconnectivity between the amygdala and other brain regions in deteriorated patients.

**Fig. S11.** Hypoconnectivity between the hippocampus and other brain regions in deteriorated patients.

**Fig. S12.** Hypoconnectivity between the pallidum and other brain regions in deteriorated patients.

**Fig. S13.** Hypoconnectivity between the putamen and other brain regions in deteriorated patients.

**Fig. S14.** Hypoconnectivity between the putamen and other brain regions in preserved patients.

**Fig. S15.** Positive correlation between functional connectivity and cognitive decline.